International Multidisciplinary Research Journal 2011, 1/2:20-26
ISSN: 2231-6302
Available Online: http://irjs.info/
IRMJ-Geology

Field characteristics and geochemistry of pyroxenite and gabbro from Odhimalai and Thenkalmalai hillocks of Bhavani ultramafic complex- South India

***K. Anbarasu, Ali Mohammed Dar, A. Karthikeyan, D. Prabhu**

Department of Geology, Periyar University, Salem, Tamilnadu-636011, India

Abstract:
The present study includes documentation of detailed geological field characteristics, petrography and geochemistry of mafic and ultramafic rocks associated with Odhimalai and Thenkalmalai hills of Bhavani complex. The lithologies well exposed in these two hillocks including Dunite, Pyroxenite, Gabbro, displaying layered arrangement comprising (from basement upwards) dunite, peridotite, pyroxenite and anorthosite-gabbro. The geochemical signatures of the gabbro and pyroxenites show a significant variation in major and trace element concentration. The pyroxenites show SiO_2 composition ranging from 49.6-55.5%, Al_2O_3 from 6-13.6%, MgO from 3.6-14.3%, CaO from 8.4-15.5% and TiO_2 from 0.24-1.7% while average composition of SiO_2, Al_2O_3, MgO, CaO and TiO_2 in gabbro varies (in %) from 49.9-58, 9.4-13, 7.4-13.1, 9-13.4 and 0.26-0.54 respectively.

Keywords: Bhavani, layered complex, Geochemistry, LREE, LILE, Petrogenesis

INTRODUCTION

The southern Indian granulite terrain is a collage of crustal blocks exposing mid – and lower levels of the continental crust, and dissected by large, intra-continental Proterozoic shear zones and lineaments, namely, the Moyar-Bavani Shear Zone, Palghat-Cauvery Shear Zone and the Achankovil Lineament. Anorthosite bearing layered complexes is common features of many Archean granulite – gneiss terrains and their emplacement relates to long term cycle of assembly and break – up of Precambrian supercontinents. Sittampundi and Bhavani layered meta - anorthosite complexes occur as tectonic lenses within the Cauvery shear zone (CSZ). The present study includes documentation of detailed geological field characteristics, petrography and geochemistry of mafic and ultramafic rocks associated with Odhimalai and Thenkalmalai hills of Bhavani complex (Fig. 1, 1a). Odhimalai is a bi-symmetrical hillock with an altitude of 654 above MSL and elevated about 250m from the base of the hill. The Thenkalmalai is a linear ridge with an altitude of ~ 389 above MSL. Both of the hillocks are striking ENE – WSW directions.

Fig.1. Panoramic view of the Odhimalai hillock.

Fig.1a. Panoramic view of the South west of Thenkalmalai hillock

Geological Setting

The lithologies well exposed in these two hillocks including Dunite, Pyroxenite, Gabbro, displaying layered arrangement comprising (from basement upwards) dunite,

Received: April 19, 2011; Revised May 30, 2011; Accepted June 01, 2011.

*Corresponding Author, Tel: +919944516378
Email: mtekali@gmail.com

peridotite, pyroxenite and anorthosite-gabbro. The geological map of the study area is given in Fig. 2. The rocks are metamorphosed and overlie on Bhavani gneiss. Most of the mafic rocks are garnetiferous indicating its participation in the regional metamorphism. Micaceous amphibole rich rocks were found as enclaves while coarse grained pyroxenites were observed in between mafic rocks. The light colored anorthositic gabbro is medium to fine grained with mafic segregations. They show a flat E-W trending linear bodies showing sub-parallelism to the trend of main shear. The pyroxenites in the complex occur as a thin lenses and bands where as some outcrops shows moderate thickness. The ultramafic and mafic association in the study area shows a dissected pattern. The rocks show a granoblastic polygonal microtexture and display disequilibrium textures (like symplectitic coronas) mostly in metagabbroic rocks containing garnet (Subramanian 1956, Janardhan and Leake, 1975; Selvan 1981; Rao, 1996). Overprinting by retrograde hydrous minerals such as amphibole, clinozoisite and biotite is prominent. Relict primary igneous textures and structures such as cumulate and compositional phase layering have been recognized in places permitting reconstruction of a generalized internal magmatic stratigraphy (Selvan, 1981). Pyroxenite and Gabbro are the two important mafic – ultramafic rock types on which main consideration will be given in the present study.

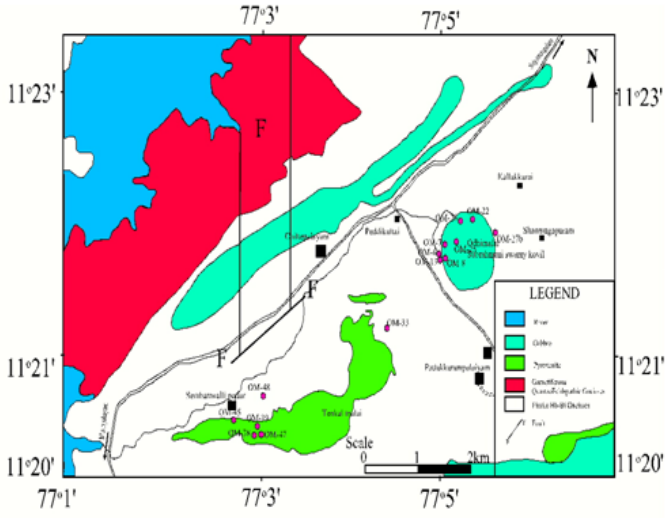

Fig. 2. Geology and Sample Location Map of the Study Area (Source: Geological Survey of India -1993)

FIELD RELATIONSHIPS

Meta –Gabbro:

This lithology is interpreted to be part of the anorthositic intrusive suite. Macroscopically, the Meta -gabbros are characterized by color indices ranging from approximately 65 to 95, with the mafic minerals being dominated by pyroxene, amphibole, and garnet. Plagioclase feldspar is the dominant light colored mineral in these rocks. Magnetite and ilmenite can also be readily identified in hand sample. These rocks often have distinctive garnet segregations—bands or blobs of garnet that can be several centimeters in width. All of these rocks are strongly deformed and metamorphosed and show consistent gneissic banding. Some of these rocks are quite dense and heavy. Colors range from dark grey to green-gray and grain sizes range from very coarse to fine. (Fig. 3) show representative photos of this rock type. The mafic bands meanwhile have an average grain size of only a couple of millimeters. The plagioclase feldspar crystals seem to preferentially resist weathering leaving a slightly bumpy and more plagioclase rich weathered surface, whereas the hand samples tend to be much darker, especially on freshly cut surfaces. .

Fig.3. Field photograph showing the Meta Gabbro

Anorthositic Gabbro

The second most abundant rock type observed in the field area is a metaanorthositic gabbro—an intermediate phase between the meta-ferro-gabbro and the metagabbroic anorthosite. In the field and in hand sample these rocks have color indices that range from approximately 40 to 65. These rocks are characterized by dark colored bands dominated by fine grained pyroxene, amphibole, and garnet and the presence of plagioclase megacrysts. The megacrysts are up to 2cm across and are altered visibly to epidote in many cases. As seen with the megacrysts in the meta-gabbroic anorthosite, these megacrysts also disrupt the overall trend of the fabric and the strongly foliated mafic bands typically deflect around the larger grains. The mafic bands meanwhile have an average grain size of only a couple of millimeters. The plagioclase feldspar crystals seem to preferentially resist weathering leaving a slightly bumpy and more plagioclase rich weathered surface, whereas the hand samples tend to be much darker, especially on freshly cut surfaces. Colors of these rocks range from dark grey to greenish grey to greenish chalky white where there is an abundance of plagioclase feldspar megacrysts. The meta-anorthositic gabbros also contain enough magnetite and ilmenite that these minerals can be easily detected. A representative photo of this rock type is shown in (Figure 4).

Fig. 4. Spheroidal weathering displayed in the Anorthosite Gabbro lithology

Pyroxenite

In Odhimalai, the pyroxenite occurs all along its eastern margin and is surrounded by the supracrustal granitic gneiss. In Thenkalmalai the pyroxenite occurs as a dominant lithology and shows layered field relationships with gabbroic litho unit. The color index of the pyroxenite generally > 90% and displays green to dark green hue for clinopyroxene and pink for orthopyroxene. Comparing grain size the pyroxenites at both the location are medium to coarse grained (Fig.5). The fine grained pyroxenites form the important litho unit in Odhimalai Hill where as the coarse grained pyroxenites are mostly observed in the Thenkalmalai hillock. In Thenkalmalai area pyroxenite and gabbro shears equal proportion where as in Odhimalai the gabbro is dominant over the pyroxenite. At places, pyroxenite is highly weathered and strained with yellowish tint. Parallel fractures filled with felsic material are common within the pyroxene bands in the Thenkalmalai sector. The pyroxinites with in the few meter range shows variation in their grain size, which varies from the very coarse to fine grained**.** A dark green colored pyroxenite layer occurs vertically in the Thenkalmalai sector where it occupies the southwestern margin of the hillock. Pyroxenite bands of cm thickness are present within in the granitic gneissic rocks. Pyroxenite rocks are asymmetrically folded with cross-criss cutting of veins. The contact between the pyroxenite and surrounding granitic gneiss at Thenkalmalai sector is shown in Fig.6.

Fig.5. Coarse grained pyroxenite displays green to dark green hue

Fig.6. Contact between the pyroxenite and surrounding granitic gneiss at thenkalmalai sector.

Petrography

Petrographic analysis was performed on the Pyroxenite and gabbro lithologies of the Odhimalai and Thenkalmalai sectors. Twelve thin sections were prepared from the rock samples collected during the field work. On each of the thin sections, mineral identifications were performed. The petrographic descriptions of these lithologies reveal the mineral content, micro textural relationships between the grains and deformational as well as alteration structures. In textural terms the rock predominantly presents cumulate texture. Pyroxenite contains clinopyroxene and orthopyroxene in more or less equal proportion exhibiting cumulous texture. Both clino – and orthopyroxenes have exsolution lamellae. Plagioclase is generally absent. Alteration of clinopyroxene into amphibole is very common. Fractured present in the clinopyroxene is filled with iron oxide. The accessory phase being the magnetite and ilmenite, concentrated characteristically along the grain boundaries. In thin section gabbro is relatively plagioclase poor, with average plagioclase abundances of 10 to 20%. A representative sample OM-13 is composed dominantly of Ortho and Clino pyroxenes with subhedral crystals of amphibole. Orthopyroxene is typically coarse grained and is characterized by subhedral crystal surface provided indication of magmatic origin. The plagioclase is mainly equigranular; medium grained and display polygonal texture with angular crystal margins.

Geochemistry:

The Major, Trace, and rare earth element (REE) geochemistry of the pyroxenites and gabbro collected from the well exposed outcrops near the Odhimalai and Thenkalmalai areas of this complex are presented in this paper.

Total of sixteen representative samples, seven are pyroxenites and nine are gabbro were analyzed for bulk chemistry at National Geophysical Research Institute (NGRI) Hyderabad. Major elements were determined by X-ray fluorescence Spectrometry (XRF) using Philips MAGIX PRO Model 2440. Trace and REE elements were analyzed by Inductive Coupled Plasma mass Spectroscopy (ICP-MS) using a Perkin Elmer SCIEX ELAN DRC II.

The geochemical signatures of the gabbro and pyroxenites show a significant variation in major and trace elements. The SiO_2 abundance covers a narrow compositional range: Pyroxenites (49.6-55.5wt %), Gabbro (50.1-58wt %). The gabbro are characterized by low TiO_2 (0.26-0.54wt %). Where as the pyroxenites shows slight concentration of TiO_2 (0.24-1.7wt %). MgO content varies from (7.4-13.1wt %) in gabbro and (3.6-14.3wt %) in pyroxenites. Major, Trace, and rare earth element (REE) concentration are given in **(Table 1).**The pyroxenites shows a high concentration of Total iron (8.4-16wt %), MgO (3.6-14.3wt %) with moderate enrichment of TiO_2 (0.24-1.7wt %) and depleted alkalies Na_2O (0.39-2.5wt %); K_2O (0.03-1.5wt %). Relative to primordial mantle the pyroxenites and gabbro shows the enriched trend in SiO_2, TiO_2, Total iron, CaO, Na_2O, and depleted trend in MgO. **(Table1).**

Table 1 Representative Major (wt %) and trace (ppm) element composition of Gabbro and Pyroxenites from Thenkalmalai and Odhimalai (Mettupailium Ultramafic complex), Tamilnadu, South India

Rock Type	Gabbro									Pyroxenite							
Sample No	OM-06	OM-07	OM-08	OM-13	OM-22	OM-23	OM-25	OM-33	OM-48	OM-32	OM-37	OM-38	OM-39	OM-40	OM-45	OM-52	PM*
SiO_2	51.5	52.3	50.1	51.5	58	53.5	54	54	49.9	55.5	51.8	52.6	51.4	51.8	49.6	53.9	45.96
TiO_2	0.36	0.41	0.35	0.37	0.32	0.3	0.26	0.39	0.54	0.88	0.65	0.24	1.7	0.42	0.58	0.45	0.18
Al_2O_3	11.0	12.8	9.4	9.7	9.9	12.4	11.5	12	13	13.1	13.6	8.4	10.6	13.7	13	6	4.06
Fe_2O_3	10.4	10.7	16.9	16.2	11.2	11.4	15	10.3	13.9	13.5	16	8.4	15.4	11.8	12.6	15.8	7.54
MnO	0.16	0.15	0.25	0.16	0.12	0.13	0.12	0.13	0.18	0.19	0.21	0.11	0.19	0.17	0.13	0.23	0
MgO	11.9	10.0	13.1	10.2	11.1	11.3	7.4	12.1	9	3.6	6.5	14.3	6.6	8	10.3	7.9	37.78
CaO	13.4	12.2	9	10.6	8.7	10.4	11.2	10.4	12.1	10.9	8.4	15.5	12.6	12.7	10.3	15.1	3.21
Na_2O	1.1	1.3	0.76	1	0.41	0.41	0.41	0.55	1.3	1.9	2.5	0.39	1.2	1.2	1.7	0.53	0.33
K_2O	0.08	0.11	0.10	0.20	0.08	0.07	0.08	0.11	0.06	0.32	0.13	0.05	0.24	0.09	1.5	0.03	0
P_2O_5	0.02	0.03	0.02	0.03	0.01	0.02	0.01	0.01	0.03	0.07	0.08	0.01	0.06	0.03	0.24	0.02	0
Total	**99.92**	**100**	**99.98**	**99.96**	**99.84**	**99.93**	**99.98**	**99.99**	**100**	**99.96**	**99.87**	**100**	**99.99**	**99.91**	**99.95**	**99.96**	**99.06**
Sc (ppm)	44.9	43.2	45.7	47.3	45.6	52.5	46.5	47.3	46.8	9.9	8.9	8.6	7.7	8.5	8	7.9	
V	195.2	205.5	219.3	235.3	304.1	180.2	222.3	260.5	242.7	298.6	286.5	288.3	263	307.7	309.4	273.7	
Cr	957.6	1683.2	1240.3	1188.4	82.6	2291.9	12007.5	546.1	778.9	21200.4	10690.4	12720.9	13342.2	11503	11938	9877.1	
Co	44.6	75.7	53	54.3	49.6	57.3	53.2	55.8	49.5	111.5	102.5	108.7	104.4	106.1	94.1	87.1	
Ni	188.6	249.4	196.7	186	81.6	305	192	151.7	163.3	1055.4	894.5	1016.5	990.5	851.3	676.8	1013.4	
Cu	35.3	33.9	23.7	26.9	21.4	19.1	39.9	34.5	30.2	60.7	66.3	59	115.7	34.8	90.2	78	
Zn	42.8	51.0	38.7	50.4	45.9	52.3	66.7	51.7	53	72.3	57.4	73.8	83	59.4	64.2	46.6	
Rb	1.7	2.5	3.5	1.4	1.4	1.6	1.5	1.5	2.8	16.4	9.7	4.4	6	4.3	11.2	5.5	
Sr	6.3	4.8	4.6	5.2	4.9	1.4	4.6	4.1	2	0.57	0.71	0.44	0.53	0.37	0.39	0.94	
Y	0.33	0.30	0.36	0.42	0.53	0.27	0.40	0.50	0.5	1.9	2.2	2.1	1.7	2.2	2.4	2.1	
Zr	0.12	0.11	0.17	0.16	0.11	0.16	0.15	0.15	0.16	0.27	0.32	0.27	0.24	0.37	0.3	0.28	
Nb	0.25	0.42	0.31	0.28	0.75	0.22	0.35	0.25	0.34	3.7	4.4	4.3	4.3	4.7	4.8	4.8	
Ba	18.7	6.7	4.9	3.9	7.7	4.0	4.4	3.1	5.2	19.6	6.6	8	5.8	6.8	7	8.2	
Hf	0.18	0.14	0.22	0.21	0.23	0.18	0.22	0.22	0.24	0.42	0.43	0.45	0.36	0.55	0.49	0.46	
Ta	0.04	0.07	0.04	0.04	0.10	0.03	0.05	0.03	0.04	0.01	0.04	0.05	0.08	0.02	0.02	0.15	
Th	0.17	0.22	0.07	0.07	0.07	0.09	0.09	0.07	0.13	1.3	1.2	1.5	1.03	1.2	0.72	2.7	
U	0.09	0.07	0.05	0.0	0.12	0.19	0.15	0.11	0.18	0.13	0.05	0.21	0.1	0.08	0.1	0.25	

PM*=Primordial Mantle Major Oxides data after Hofmann, A.W. (1988).
Fe_2O_3= Total Iron as Fe_2O_3

Table 1 (continued) Rare earth element composition

	OM-06	OM-07	OM-08	OM-13	OM-22	OM-23	OM-25	OM-33	OM-48	OM-32	OM-37	OM-38	OM-39	OM-40	OM-45	OM-52
La (ppm)	2.53	1.63	1.48	1.35	2.50	1.37	1.26	0.93	1.21	1.16	1.02	1.28	0.83	1.30	1.05	1.15
Ce	4.46	3.88	3.74	3.34	5.62	2.83	3.17	2.33	2.92	2.93	2.91	2.94	2.26	3.40	3.08	2.88
Pr	0.56	0.56	0.53	0.48	0.82	0.42	0.54	0.42	0.47	0.34	0.34	0.37	0.28	0.38	0.39	0.36
Nd	3.01	3.23	2.89	2.85	4.95	2.50	3.34	2.86	3.14	1.71	1.91	1.83	1.46	1.94	2.08	1.82
Sm	0.94	0.89	0.86	0.92	1.49	0.74	1.06	1.06	1.08	0.44	0.48	0.45	0.38	0.50	0.52	0.45
Eu	0.37	0.30	0.33	0.38	0.59	0.26	0.36	0.41	0.37	0.12	0.13	0.12	0.11	0.14	0.14	0.12
Gd	1.18	1.01	1.03	1.28	1.75	0.87	1.21	1.40	1.46	0.79	0.85	0.89	0.67	0.89	0.95	0.89
Tb	0.20	0.16	0.19	0.23	0.29	0.16	0.21	0.27	0.27	0.16	0.17	0.18	0.14	0.20	0.20	0.18
Dy	1.54	1.24	1.45	1.80	2.20	1.18	1.66	2.12	2.01	1.38	1.48	1.49	1.18	1.55	1.71	1.49
Ho	0.35	0.27	0.32	0.39	0.50	0.26	0.36	0.48	0.47	0.35	0.38	0.37	0.31	0.39	0.44	0.38
Er	0.98	0.79	0.90	1.10	1.32	0.71	1.01	1.31	1.29	1.12	1.26	1.21	1.02	1.28	1.43	1.26
Tm	0.13	0.10	0.12	0.14	0.17	0.09	0.13	0.17	0.16	0.18	0.21	0.19	0.17	0.20	0.23	0.20
Yb	0.76	0.59	0.71	0.81	1.05	0.51	0.76	1.01	0.98	1.20	1.42	1.26	1.13	1.33	1.51	1.31
Lu	0.16	0.13	0.16	0.18	0.23	0.11	0.17	0.22	0.22	0.21	0.25	0.24	0.20	0.25	0.26	0.23
Pb	6.08	5.9	6.10	4.20	5.17	4.71	5.19	5.29	5.96	0.01	0.02	0.01	0.02	0.01	0.01	0.01
ΣREE	17.17	14.78	14.71	12.25	23.48	12.01	15.24	14.99	16.05	12.08	12.81	12.83	10.13	13.75	13.99	12.73
CeN/YbN	1.58	1.77	1.42	1.11	1.44	1.49	1.13	0.62	0.80	0.66	0.55	0.63	0.54	0.69	0.55	0.59
LaN/SmN	1.68	1.14	1.07	0.91	1.04	1.15	0.74	0.54	0.70	1.66	1.32	1.76	1.35	1.62	1.25	1.58
GdN/YbN	1.28	1.41	1.19	1.30	1.37	1.41	1.31	1.14	1.23	0.54	0.49	0.58	0.49	0.55	0.52	0.56
Eu/Eu*	1.06	0.96	1.06	1.06	1.11	.98	0.96	1.02	0.89	0.62	0.61	0.57	0.65	0.63	0.60	0.57
Rb/Nb	7.51	6.69	12.69	5.76	2.14	8.03	4.71	6.65	9.31	4.97	2.48	1.14	1.54	1.03	2.64	1.27
Th/Nb	5.71	4.38	1.90	2.10	0.78	3.41	2.16	2.34	3.18	2.95	2.24	2.91	1.98	2.15	1.26	4.67

Bulk composition/whole rock analyses indicate that the magma type is tholeiitic but trending towards a calc-alkaline nature also supported by AFM diagram (Irvin and Banger) **(Fig. 7)**. Jenson (1976) cation plot uses Al_2O_3, FeO(t) +TiO_2 and MgO cations because of the stability of these elements during metamorphism. The plot **(Fig. 8)** indicates that most of the samples cluster on the border of high-Fe (HFT) and high-Mg (HMT) tholeiitic basalt. Some of the samples are Mg-rich and plot in the basaltic komatiitic (BK) field. Based on the TiO1, MnO, P_2O_5 triplot (proposed by Mullon 1983) most of the samples fall within the Calc-alkaline basaltic (CAB) field **(Fig. 9).** Thus it could be inferred that the tectonic environment of eruption is volcanic arc environment and the studied sample falls within the Calc-alkaline basaltic field. Concentration of compatible trace elements in pyroxenites like V (273.7-309.4ppm), Cr (9877.1-13342.2ppm), Co (87.0-111.5ppm) and Ni (676.8-1055.4ppm) are high while these pyroxenites are poor in incompatible and HFS elements like Rb, Hf, Ta, Th, and U. Sr shows a remarkable low concentration ranging from (0.37-0.94wt%). Similar pattern are observed in gabbro samples being enriched in compatible trace elements and poor in incompatible and HFS elements. Total REE value of pyroxenites varies from (10.13-13.99ppm) with limited REE, (Ce_N/Yb_N= 0.55-0.69) and LREE fractionation (La_N/Sm_N= 1.32-1.66). The HREE also conclude limited fractionation (Gd_N/Yb_N= 0.49-0.58) with negative Eu anomaly.

For the gabbro samples the total REE also shows a fractionation with in a limited range. The total REE values varies from (12.01-23.48ppm) with limited REE fractionation (Ce_N/Yb_N= 0.62-1.77). LREE (La_N/Sm_N= 0.54-1.68) and HREE fractionation is also within limited range (Gd_N/Yb_N =1.19-1.37) with negligible Eu anomaly.

Condritic normalized REE plot (after Sun and McDonough (1989) of pyroxenites reflects negative Eu anomaly with slight enrichment of HREE **(Fig. 10).** The negative Eu anomaly in these samples may be interpreted as due to fractionation of plagioclase ± hornblende and can be

imposed when the melt phase enters the stability field of plagioclase. The Low LREE and slight enriched trend of HREE may be retained some what by clinopyroxenes or to a greater extent by hornblende.

The condritic normalized REE plot of gabbro shows a flat REE pattern with gentle or without any Eu anomaly **(Fig. 11).** The flat REE pattern in association with low CaO, Al_2O_3 , Sr content and absence of Eu anomaly all of these features suggests removal of plagioclase component from basic parent magma or may be due to the magma that might have segregated at such depth where plagioclase is not stable and hence it could not be fractionated (Barker et al., 1976).

The representative primitive mantle normalized trace element plot (after Sun and McDonough (1989) for pyroxenites and gabbro are presented in **(Fig. 12).** Relative to primitive mantle (and also in comparison with MORB, both the set of rocks shows the relative enrichment of LILs and LREEs. They are further characterized by a low Th abundance and a distinct Nb-Ta, Zr-Hf trough. These features are characteristic of tholeiitic basalts produced at destructive plate margins or within plate tholeiites contaminated by continental crust (Hawkesworth et al., 1994).

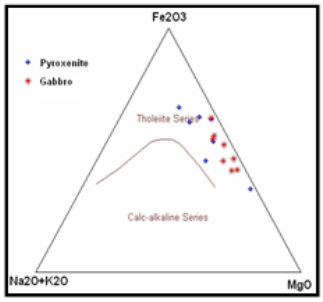

Fig. 7 AFM diagram for gabbro and pyroxenites (after Irvin and Baragar, 1975)

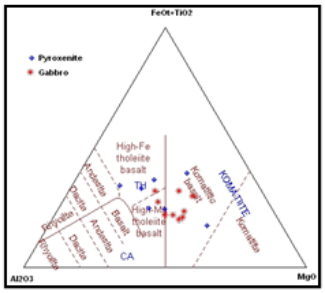

Fig. 8 Jensen's cation Plot for Gabbro and Pyroxenite (after Jensen 1976)

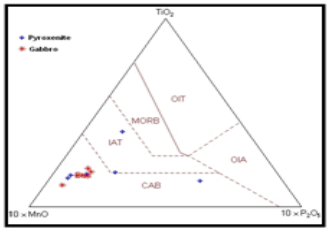

Fig. 9 TiO2-MnO-P2O5 triplot for Gabbro and Pyroxenite. (after Mullen 1983)

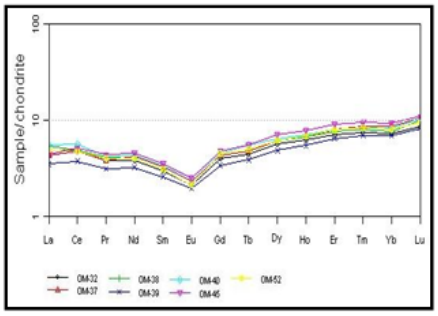

Fig.10. Chondrite normalized REE diagram for the Pyroxenites after Sun and McDonough (1989)

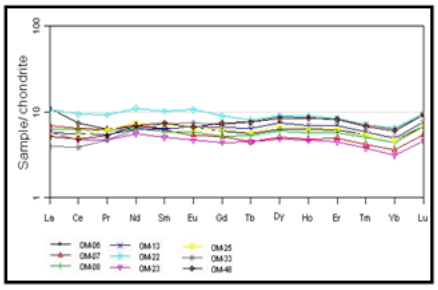

Fig. 11. Chondrite normalized REE diagram for the Gabbro from Bhavani ultramafic complex normalized after Sun and McDonough (1989)

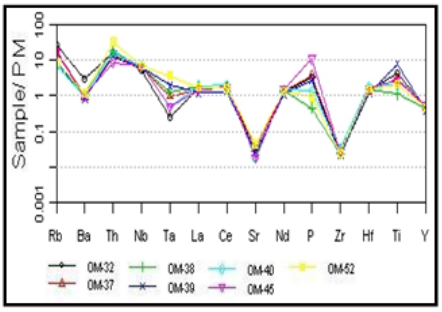

Fig. 12. Primitive Element-normalizes multi-element diagram for Pyroxenites after Sun and McDonough (1989).

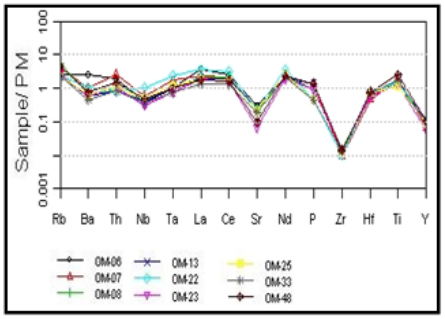

Fig. 12 a. Primitive Element-normalizes multi-element diagram for Gabbro after Sun and McDonough (1989).

Tectonic Setting

The geochemistry of mafic and ultramafic rocks is most commonly used to discriminate tectonic setting. The idea of trying to fingerprint magmas from different tectonic setting chemically is best attributed to Perace and Cann (1971, 1973). These authors show that it is a possible to use geochemistry to

distinguish between basalts produced in different, known tectonic settings. The basaltic rocks are formed in almost every tectonic environment and they are believed to be geochemically sensitive to the changes in plate tectonic frame work. In order to understand the tectonic environment of the studied samples the plot Ti/1000 &V (after Shervais, 1982) shown in **(Fig. 13)** depicts that the studied samples fall in the Arc tholeiitic environment.

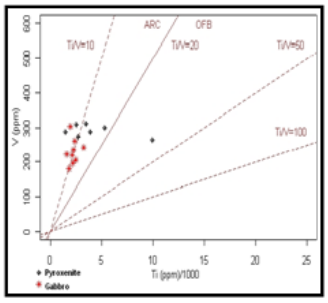

Fig. 13 Ti/1000 Vs V tectonic discrimination diagram (after Shervais 1982) for Gabbro and Pyroxenite

CONCLUSION

The geochemical constraints of the gabbroic rocks and pyroxenites of the Bhavani complex suggest island arc magmatism. The major element relations of the gabbro and the pyroxenites suggest tholeiitic to calcalkaline signatures of typical island arc environment. They are further characterized by a low Th abundance and a distinct Nb-Ta, Zr-Hf trough. These features are characteristic of tholeiitic basalts produced at destructive plate margins or within plate tholeiites contaminated by continental crust. The studied samples show enriched nature of LILE and depleted trend in HFSE. The –ve Eu anomaly observed in the pyroxenite samples signify the role of plagioclase fractionation in their petrogensis.

ACKNOWLEDGEMENTS

The authors are thankful to Department of Science and Technology for providing financial support. We acknowledge the help received from Mr. Sariput Sawant during geochemical analysis at National Geophysical Research Institute Hyderabad (NGRI).

REFERENCES

Ahmad T, Tarney J. 1994. Geochemistry and petrogenesis of late Archean Aravalli volcanics, basement enclaves and granitoids, Rajasthan. Precambrian Res 65:1–23.

Akhtar R Mir, Shabber H Alvi, and Balaram V, 2010. Geochemistry of the mafic dykes in parts of the Singhbhum granitiod complex: petrogenesis and tectonic setting. Arab J Geosci doi: 10.1007/s1251701001216.

Balaram V, and Rao TG. 2003. Rapid determination of REE and other trace elements in geological samples by microwave acid digestion and ICP-MS. Atom. Spectrosc 24:206–212.

Barker F, Arth JG, Peterman ZE, and Friedman. I. 1976. The 1.7 to 1.8-b.y. old trondhiemites of south western Colorado and northern new mexico. Geochemistry and depth of genesis. Geol Soc Am Bull 87:189-189.

Brique L, Bougault Joron JL. 1984. Quantification of Nb,Ta,Ti,and V anomalies in magamas associated with Subduction zones: petrogenitic implication. Earth and planetary Science Letters 68:297-308.

Dungan MA, Rnodes JM. 1978. Residual glasses and melt inclusions in basalts from DSDP Legs 45 and 46: evidence for magma mixing. Contrib Mineral Petrol 67:417–431.

De Paolo DJ. 1981. Trace element and isotopic effects of combined wallrock assimilation and fractional crystallization. Earth Planet Sci Lett 53:189–202.

Dessai AG, Arolkar DB, French D, Viegas A, and VISWANATH TA. 2009. Petrogensis of the Bondla Layered Mafic-Ultramafic complex, Usgaon, Goa. Jour Geo Soc India 73: 697-714.

Hoffmann AW. 1988. Chemical differentiation of the earth: the relationship between mantle, continental crust and oceanic crust. Earth planet Sci Lett 90:297-314.

Hawkesworth CJ, Gallagher AK, Hergt JM, and Mcdermott, BF. 1994. Destructive plate margin magmatism: Geochemistry and melt generation. Lithos 33:169-188.

Irvine TA, Baragar WRA. 1975. A guide to the chemical classification of the common volcanic rocks. Canadian Journal of Earth Sciences 8:523-546.

Janardhan AS, and Leake BE. 1975. The origin of meta-anorthositic gabbros and garnetiferous granulites of the Sittampundi complex, Madras, India. J Geol Soc India 6:391-408.

Jensen LS. 1976. A new cation plot for classifying subalkalic volcanic rocks. Min Nat Resources Ontario Division of Mines Misc paper 66:20.

Kepezhinskas P, Mcdermott F, Defant MJ, Hochstaedter A, Drummond MS, Hawkesworth CJ, Koloskov A, Maury RC, Bellon H. 1997. Trace element and Sr–Nd–Pb isotopic constraints on a three component model of Kamchatka arc petrogenesis. Geochim Cosmochim Acta 61:577–600

Krishna AK, Murthy NN, and Govil PK. 2007. Multielement analysis of soils by wavelength-dispersive X-ray fluorescence spectrometry. Atom Spectrosc 28:202-214.

Middlemost EAK. 1994. Naming materials in the magma/igneous rock system. Earth-Science Rev 37:215-224.

Mullen ED. 1983. MnO/TiO2/P2O5: a minor element discriminant for basaltic rocks of oceanic environments and its implications for petrogenesis. Ear Planet Sci Letters 62:53–62.

Mistafa M Hariri, 2004. Petrographical and geochemical characteristics of the ultramafic rocks of Jabal zalm, central arabian shield, Saudi Arabia. The arabian Jour for Science and Engineering. 29:123-132.

Rao YJB, Chetty TRK, Janardhan AS, and Gopalan K. 1996. Sm-Nd and Rb-Sr ages and P-T history of the Archean Sittampundi and Bhavani layered meta-anorthosite complexes in Cauvery shear zone, South India: evidence for Neoproterozoic reworking of Archaean crust. Contrib Mineral Petrol 125:237-250.

Rollinson H. 2008. Secular evolution of the continental crust: Implications for crust evolution models. Geochem Geophy Geosystems (G3) 9 (12):1-14.

Santosh M, Maruyama S, and Sato K. 2009. Anatomy of a Cambrian: Pacific-type orogeny in Southern India. Gondwana Res 16:321-341.

Selvan TA .1981. Anorthosite-gabbro-ultramafic complex around Gobichettypalayam, Tamil Nadu and their possible relation to Sittampundi type anorthosite complex (unpublished). Ph.D. thesis Univ Mysore Mysore India.

Subba Rao MV, and Srikanth B. 2004. Major,Trace and platinum group elements(PGE) geochemistry of the pyroxenites of Mettupalaiyam ultramafic complex, Tamil nadu. Journal of applied geochemistry 6:190.197.

Subramanian AP. 1956. Mineralogy and petrology of the Sittampundi complex, Salem district, Madras state, India. Bull Geol Soc Am 67:317-390.

Sun S, and Mcdonough WF. 1989. Chemical and isotopic systematic of oceanic basalts: implications for mantle composition and processes. *In*: A.D.Saunders and M.J.Norry (Eds.), Magmatism in the ocean basins. Geol Soc London Sp Pub 42:313-345.

Shervais JW. 1982. Ti-V Plots and Petrogenesis of modern and ophiolitic Lavas. Earth Planet Sci Lett 59:108–118.

Taylor SR, Mclennan SM. 1985. The continental crust: its composition and evolution. Blackwell, Oxford.

Verma SP. 2006. Extension-related origin of magmas from a garnetbearing source in the Los Tuxtlas volcanic field, Mexico. Int J Earth Sci (Geol Rundsch) 95:871–901.

Weaver BL, Tarney J. 1983. Chemistry of the sub continental mantle inferences from Archean and Proterozoic dykes and continental flood basalts. In: Hawkesworth CJ, Norry MJ (eds) Continental Basalt and Mental Xenoliths. Shiva Nantwich :209–229.

Windley BF, and Smith J.V. 1976. Archaean high grade complexes and modern continental margins. Nature 260:671-675.

Yellappa T, Chetty TRK, Tsunogae T, and Santosh M. 2010. The Manamedu Complex: Geochemical constraints on Neoproterozoic suprasubduction zone ophiolite formation within the Gondwana suture in south India. J Geodyn doi:10.1016/j.jog.2009-12.004.